Aqueous Self-assembly of Peptide-Diketopyrrolopyrrole Conjugates with Variation of N-alkyl Side Chain and π-Core Lengths

Sayak Subhra Panda[a]

John D. Tovar*[a,b]

[a] Department of Chemistry, Johns Hopkins University, 3400 North Charles Street, Baltimore, Maryland 21218, United States.

[b] Department of Materials Science and Engineering, Johns Hopkins University, 3400 North Charles Street, Baltimore, Maryland 21218, United States

* indicates the main/corresponding author.

tovar@jhu.edu

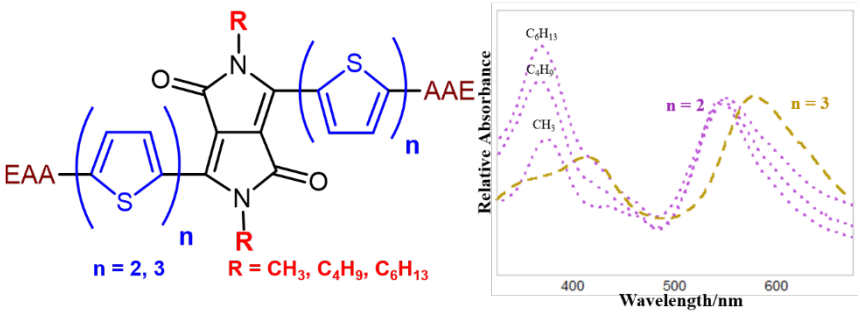

Received:
Accepted:
Published online:
DOI:

Abstract Peptidic sequences when conjugated to π-electronic groups form self-assembled networks of π-electron pathways. These materials hold promise for bio-interfacing charge transporting applications because of their aqueous processability and compatibility. In this work, we incorporated diketopyrrolopyrrole (DPP), a well-established π-core for organic electronic applications, within the peptidic sequence. We embedded different numbers of thiophene rings (2 and 3) on both sides of the DPP to alter the length of the π-cores. We also varied the length of the N-alkyl side chains (methyl, butyl, hexyl) attached to the DPP core. These variations allowed us to explicitly study the effect of π-core and N-alkyl side-chain length on photophysical properties and morphology of the resulting nanomaterials. All of these molecules formed H-type aggregates in the assembled state. Longer π-cores have relatively red-shifted absorption maxima whereas the N-alkyl variation did not present significant photophysical changes.

Key words Peptide-π conjugates - Diketopyrrolopyrroles – Aqueous self-assembly – Side-chain engineering

Introduction

Peptides are attractive motifs for the realization of self-assembling materials due to their ease of synthesis and structure/property tunability upon variation of amino acid composition. Peptides leverage intermolecular interactions such as hydrogen bonding, van der Waals and other electrostatic forces to form a diverse range of nanostructures.[1-4] Functionalizing self-assembling peptides with π-electron groups provides an attractive route to form ordered structures with long-range π-conjugated networks that can enable charge transporting field-effect transistor and solar cell applications.[5-11] These materials could also be used for biocompatible applications due to their aqueous processability. However, peptide-π electron networks vary significantly from the natural peptide systems due to the presence of non-natural π-electron systems. Hence, it is of paramount importance to understand the extent to which the peptides and pi-cores can be tuned, the structural organization that results from such variations and the specific optoelectronic and electrical properties that result.

Among different peptide-π conjugated systems, 'peptide-π-peptide' triblock materials received significant interest due to their ability to form tapelike 1-D nanostructures with high aspect ratios.[12-16] These π-peptides contain oligomeric π-electron sequences which will facilitate intermolecular quadrupole interactions (e.g. "π-stacking") while the attached peptide sequences will promote hydrogen bonding networks akin to beta-sheets and other peptide secondary architectures. Collectively, the entire ensemble can participate in more generalized electrostatic interactions such as induced dipole/van der Waals/dispersion interactions within a supramolecular assembly. A range of π-electron moieties was installed within these triblock constructs ranging from linear oligothiophenes and oligophenylenes[14, 17] to more "2-D" perylenediimide,[12] benzotrithiophene and porphyrin[18] groups. The emergent optoelectronic and electrical properties depend on the specific amino acids in the peptidic wings and on the installed π-electron groups. For example, smaller amino acid residues closer to the π-core tend to form 'tighter' assembled networks.[16] Similarly, oligothiophenes showed better charge transporting properties as compared to oligophenylenevinylenes when installed within the same peptide segment.[19] Despite the extensive research on peptide-π conjugated materials, structural orientation of the π-cores within the higher order fibrillar networks, which could be used as a design principle while selecting monomers, is still not understood comprehensively. Towards this end, we explored the incorporation of larger aromatic and aliphatic groups oblique to the peptide backbone to understand their impacts on the self-assembly process.[20, 21] For example, 'cruciform' type π-cores showed the absence of higher ordered structures, which is in line with the proposed lateral stacking model in these systems.[20]

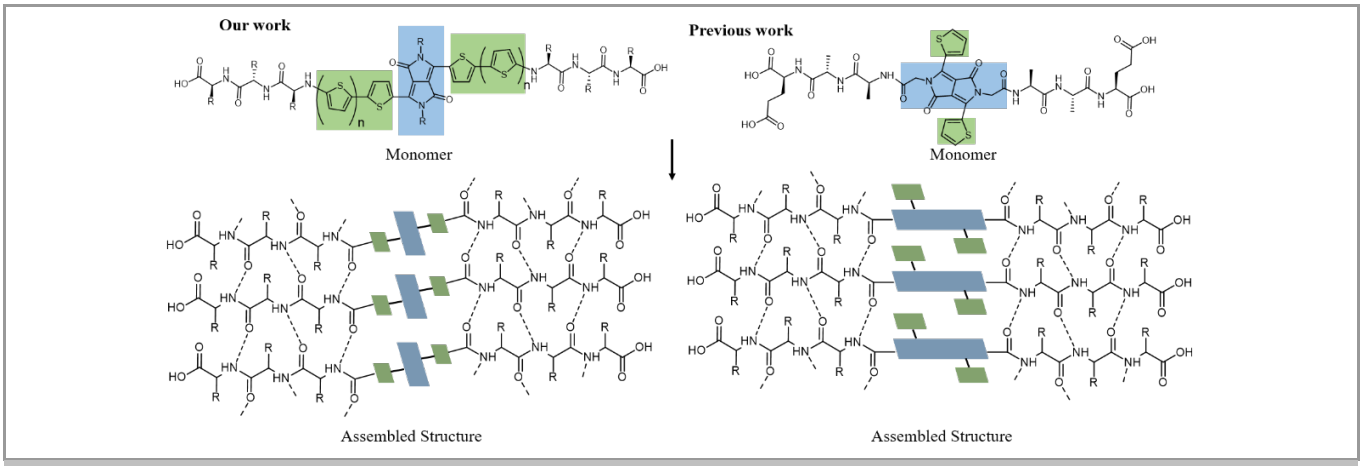

Scheme 1 Schematic representation of monomer and assembled structure of peptide-DPP conjugates.

Introduction of smaller -CH_3 groups on the oligothiophene cores also resulted in less compact H-type aggregated systems.[21] Hence, there remains a need to understand complexities of the self-assembly process through judicious design and tuning of π-cores.

To further our research on geometrically non-linear chromophores, we explored diketopyrrolopyrrole (DPP) within the peptide constructs. DPPs have favorable LUMO levels allowing for facile electron injection relevant for the design of polymer active layers for solar cells and field-effect transistors,[22-27] and they are thermally stable and photo-stable.[28] Charge delocalization properties of DPP-based molecules are attributed to the efficient π-π stacking and relatively planar structure which leads to increased intermolecular hopping in the solid state.[29, 30] Thiophene-flanked DPPs are especially attractive for charge transporting applications due to the maintenance of co-planarity resulting from less backbone torsional strain,[29] and due to the ease of synthesis and functionalization.[22, 26] However, DPP building blocks are poorly soluble in organic solvents thus requiring the installation of solubilizing groups for solution processability. which are well established to impact the optoelectronic and electrical properties.[31-36] For example, Back *et al.* identified an odd-even effect in the structure and electrical conductivities with variation of side chain length in a DPP-containing polymer.[32] Gruber *et al.* investigated the effect of linear and branched side-chains on the thin film structure and electrical properties of DPP-based polymers.[33] Examples of DPP conjugates that are processable in aqueous condition are much rarer,[37 - 43] and out of those, DPP-peptide conjugates have not been extensively explored.[37-39] Draper *et al.* prepared conductive hydrogels by conjugating phenylalanine to the amide functionalities of a thiophene-conjugated DPP-core.[37] Rani *et al.* also targeted the DPP amide functionality by conjugating an octapeptide to the DPP-core, which resulted in H-type aggregates in aqueous solution.[38]

In this work, we describe the effect of incorporating different π-conjugated core lengths in the peptide backbone as well as different N-alkyl side chain lengths oblique to the peptide backbone. This work diverges from other DPP-peptide conjugates studied previously in that the long pi-conjugation axes of the DPP oligomers are coincident with the peptide backbone directionality, while the N-atoms of the DPP cores are engaged for alkyl group substitution rather than for peptide amidation (Scheme 1). We identified that that the length of π-core has a significant effect on the subsequent optoelectronic properties while N-alkyl side chain variation only offered minute changes. This design principle offers a fine-tuning of optoelectronic properties within these nanomaterials while allowing access to one of the high-performing π-cores in aqueous media that could be used for future charge transporting applications.

Results and Discussion

Synthetic Strategy: Peptide-π-peptide triblock molecules presenting acidic amino acid residues can self-assemble under acidic conditions by leveraging the added hydrogen bonding propensity of amino acids with the π- π interactions among the central cores. In basic conditions, these molecules maintain their monomeric properties due to the presence of multiple carboxylates that are well solvated by the aqueous medium. Upon acidification, these molecules form pi-stacked fibrillar arrays with embedded π-conjugated networks. We previously identified EAA as a tripeptide sequence that, when conjugated to oligothiophene cores, resulted in 1-D nanostructures with highly efficient charge-transporting capabilities.[44] In this work, we appended the same sequence to the central DPP π-core.

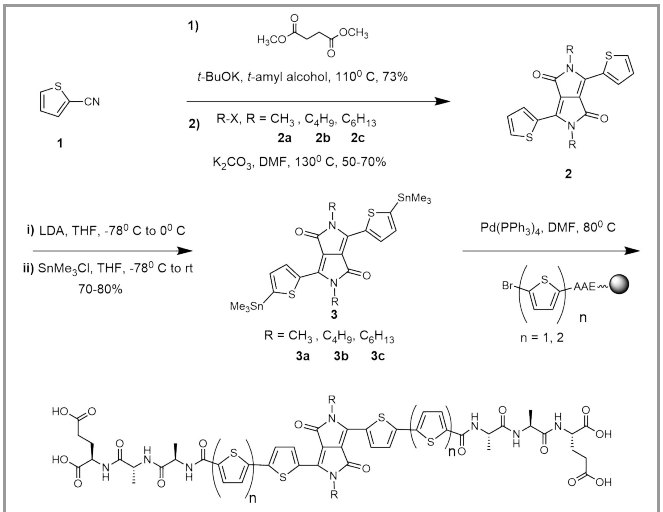

Scheme 2 Synthetic scheme of DPP-conjugated peptides.

We used Pd-catalyzed Stille couplings to incorporate the DPP π-cores into the peptide backbones. Thiophene-diketopyrrolopyrrole (TDPP) units were functionalized with stannanes on both ends to be used as a transmetallation agent for on-resin Stille coupling (Scheme 2). The resin-bound peptide sequence EAA-NH_2 was synthesized using Fmoc-based solid-phase peptide synthesis protocols. The N-acylation of the terminal amine was performed with varied length of thiophene (mono vs bi) cores which were functionalized with bromine rendering them a suitable candidate for Pd-catalyzed cross-coupling reactions. After the final coupling, the peptide-π-peptide triblock molecules were achieved. All of the peptides were synthesized using the above mentioned protocol in moderate yield (Table 1). 5'-bromo-[2,2'-bithiophene]-5-carboxylic acid and 5-bromothiophene-2-carboxylic acid were used as N-acylation agents to synthesize 3T and 2T compounds respectively. We kept the EAA tripeptide sequence constant to understand the photophysical and microscopic effect of variation of the length of side chain and of the π-core. The side chain length was varied systematically from methyl (C1), butyl (C4) to hexyl (C6) groups when two thiophene groups (2T) were attached on both sides of the DPP-core. However, we only synthesized the two extreme ends i.e. methyl (C1) and hexyl (C6) groups when three thiophene groups (3T) were attached to both sides of the DPP core.

Nanostructure Morphology: We visualized the nanostructures that formed following pH-triggered assembly using transmission electron microscopy (TEM) to probe the effect of alkyl side chain as well as length of π-core on the resulting nanostructures. The 2T compounds formed 1-D tapelike nanostructures upon assembly as evident from Figure 1a and Figure S19. These nanostructures are several hundred nanometers in length, which appear to be smaller than the previously reported 1-D nanoaggregates.[15] DLS also corroborates this idea where relatively smaller aggregates were recorded as compared to previously reported peptides (Figure S21).[15] C1-2T, C4-2T and C6-2T formed nanostructures with comparable widths of 4.1 ±0.5 nm, 3.9 ±0.8 nm, and 3.6 ±0.7 nm respectively. This shows only minor variation in lateral association of peptide fibrils. It is worthwhile to note that the length of the nanostructures appears to decrease gradually with increase in the length of the side chain alkyl group. We could not accurately measure the C4-2T and C6-2T lengths as they formed bundle-type structures as compared to the isolated tapes formed by C1-2T. 3T compounds formed relatively more random aggregates as compared to the 2T peptides as visualized by TEM (Figure 1b, Figure S20). They also appear to form bundle-type structures with relatively shorter nanostructure lengths. This shows that the length of the π-core also influences the molecular packing in these materials.

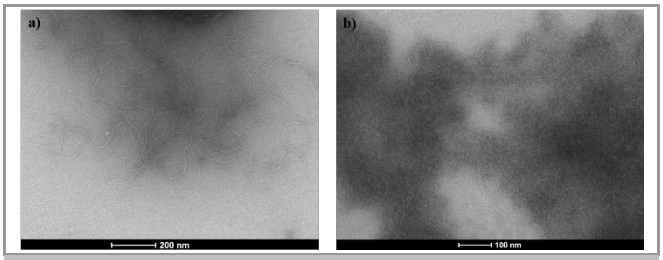

Figure 1 Representative transmission electron microscopy images of a) C1-2T and b) C1-3T under acidic medium.

Photophysical characterization: Photophysical responses were recorded for all the peptides in their assembled (pH 1) and monomeric (pH 8) states. The glutamic acid (E) present in the peptide backbone remains deprotonated in basic medium promoting effective aqueous solvation and minimizing interactions between the monomers. The peptides self-assemble under acidic medium due to the screening of localized formal charges following carboxylate protonation. UV-Vis absorption, photoluminescence and circular dichroism spectra were recorded in aqueous medium for the peptides both in the assembled and dissolved states in order to probe how inter-chromophore interaction changes as a result of self-assembly.

The UV-vis absorption spectra of all monomeric DPP-conjugated peptides exhibit two different absorption bands: one around 400 nm due to the π- π* transition of the conjugated DPP-oligothiophene unit, and one around 600 nm due to the intramolecular charge transfer (ICT) from the thiophene (donor) group to the DPP (acceptor) lactam units.[45] All of the peptides with two thiophene groups flanking the DPP (i.e. C1-2T, C4-2T and C6-2T) showed the ICT band around 586 nm and π- π* transition around 370 nm, with no variation of λ_{max} with the length of the side chains (Figure 2a). However, the relative intensity of the π- π* transition with respect to ICT transition increases with the length of the side chain. An additional shoulder around 660 nm was evident for all the 2T compounds, corresponding to the ICT within aggregated species in higher ordered thiophene-DPP conjugated molecules.[45] Indeed, DLS data acquired at basic pH (Figures S21) indicates that the π-peptides are not molecularly dissolved but rather suggest the presence of smaller aggregates which are responsible for the observed electronic couplings at basic pH. Rani *et al*. also observed a similar low-energy absorption peak in assembled DPP-peptide conjugates in aqueous solution.[38] A similar trend was also observed in the assembled state (Figure 2b), where the ICT transition around 548 nm and the π-π* transition around 370 nm remained unperturbed with the variation of the side chain. Blue-shifts of the ICT transition by around 38 nm in the assembled state point to the formation of H-type aggregates. However, we cannot rule out the possibility that the change in bulk solution polarity with pH contributes to the higher-energy shift of the ICT transition, as such solvatochromism was observed by Wilson and co-workers in a series of solvents.[46] Previously, Draper *et al*. also reported broadening of the ICT transition in H-type DPP-peptide conjugates,[37] whereas Rani *et al*. characterized the H-type aggregates by diminished intensity of the 0-0 transition relative to the 0-1 transition in DPP-octapeptide conjugates.[38] To the best of our knowledge, this is the first example of unique blue-shifts observed in DPP-peptide conjugates upon moving to the aggregated state. The prominent shoulder around 660 nm red-shifted to 690 nm possibly due to the restricted rotational motion of the chromophore with aggregation. The intensity of the π-π* transition with respect to the ICT transition also followed the same trend found in basic medium where highest intensity was observed for C6-2T and lowest for C1-2T.

For peptides with three thiophene groups (C1-3T and C6-3T), in basic media we observed the ICT peak around 612 nm and the π-π* transition around 414 nm (Figure 2c). The molecular red-shift of the π-π* transition compared to the 2T compounds results

from the extra thiophene rings conjugated onto the DPP backbone. The low energy-shoulder of the ICT band was only visible for C6-3T around 680 nm. Upon acidification, the ICT band shifted to 578 nm (blue shifted by 34 nm) and the π-π* transition remained unchanged, qualitatively similar to the 2T cases. The ICT shoulder of C6-3T red-shifted similar to the other peptides to 730 nm, the formation of which was consistent with similar terthiophene-DPP conjugated compounds.[47] We also observed visually a clear color change from blue to purple, indicative of aggregate formation as described by Reynolds and co-workers.[47] The intensity ratio of the π-π* transition to ICT transition followed the same trend as 2T molecules where C6-3T showed higher intensity as compared to C1-3T. Due to the complexity of the core, we expect this to engage in non-ideal H-type aggregation (rotationally and translationally shifted).[38] The lower intensity of π-π* transition may be due to the better H-type (parallel) aggregation of the thiophene groups in presence of the methyl group side chain as compared to longer side chains. Overall, we observed minute change in optical absorption with variation of side chain, in line with previous reports.[48] However, there is a significant difference in optical absorption with the length of the π-core, as expected.

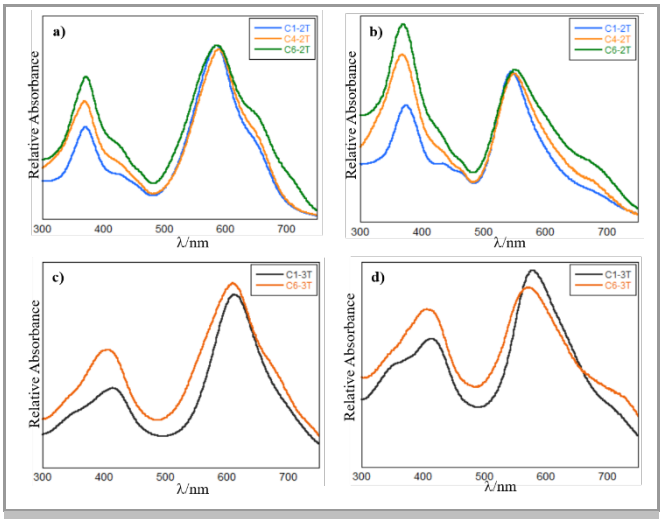

Figure 2 UV-Vis spectra of 2T-peptide conjugates in a) basic and b) acidic medium (top row). UV-Vis spectra of 3T-peptide conjugates in c) basic and d) acidic medium (bottom row). All the spectra were recorded at 5-10 μM concentration range. Basic solutions were prepared by addition of 20 μL of KOH (1M) to the spectroscopic solution in water. Acidic samples were obtained by adding 50 μL of HCl (1M) to the basic sample.

We also investigated the emission spectra of the DPP-peptide conjugates under basic (monomeric) and acidic (assembled) conditions. For all the compounds, we probed the emission signatures of both of the π-π* and ICT transitions. Although the emission signature of the ICT transition has been explored previously, reports that probe the π-π* transition in aqueous medium are not apparent. **2T** compounds exhibited a featureless broad emission maximum around 450 nm upon exciting around the π-π* transition (i.e. 370 nm) in basic solution, which remain unperturbed (shift about 1-2 nm) in wavelength with lowering of pH. The intensity of the spectra increases slightly in acidic medium. This indicates that the thiophene core region is not aligned completely parallelly (i.e. H-type) in acidic medium. The ICT transition has a relatively low quantum yield, as observed by the lower intensity of the emission spectra in basic medium (monomeric state), which is in contrast to the previous DPP-peptide conjugates studied in aqueous medium.[38] The low intensity could be attributed to the non-radiative relaxation of the ICT transition. However, we cannot rule out the possibility of assembled structures pre-existing to some extent in basic medium considering the high stacking propensity of the DPP core. The signal is completely quenched in acidic medium indicating formation of parallel H-type aggregates. A representative spectrum is shown in Figure 3a, others can be found in the supporting information.

Probing the π-π* transition of **3T** compounds also resulted in broad featureless emission profiles in basic media (Figure 3b). Upon lowering the pH, we did not observe any change in the wavelength maxima, however, the intensity decreased significantly as opposed to **2T** compounds. We anticipate that the longer π-cores resulted in formation of better parallel orientation of the oligothiophene region in the assembled state. Exciting the ICT transition did not result in any meaningful emission under basic and acidic medium. We anticipate that longer π-cores coupled with higher stacking propensity of DPP-cores form hierarchical structure already in the basic solution, similar to 2T.

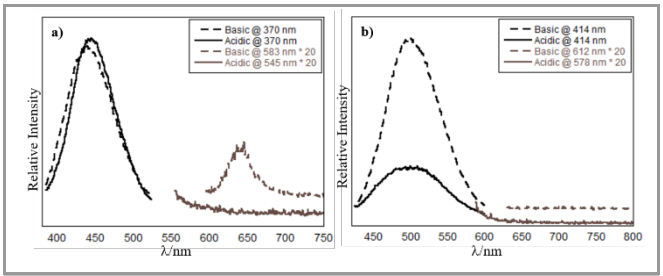

Figure 3 Emission spectra of a) C1-2T and b) C1-3T molecules in basic and acidic solutions. All the spectra were recorded at the 5-10 μM concentration range. Basic solutions were prepared by addition of 20 μL of KOH (1M) to the spectroscopic solution in water. Acidic samples were obtained by adding 50 μL of HCl (1M) to the basic sample.

CD spectroscopy informs about the local chiral chromophore environment induced by the molecular self-assembly. We monitored the exciton-coupled bisignate Cotton effect (i.e. the sign change of the CD signal due to the electronic coupling of transition dipoles of adjacent chromophores) around the π-π* and ICT transitions to understand the extent of interaction in between DPP-peptide molecules. CD spectra of 2T compounds recorded in basic environments showed sign changes around the absorption maxima of the ICT transition (i.e. 585 nm) indicating presence of exciton coupling between the chromophores. Upon lowering the pH, the crossover shifted to lower wavelength (i.e. 550 nm) in accordance with the change in λ_{max} of the ICT transition observed in absorption spectroscopy. The signal intensity also increased slightly indicating stronger interaction among chromophores. Another crossover was observed around the π-π* transition in acidic medium which was not evident in basic medium (Figure 4a). This indicates that there is a change in inter-chromophore orientation upon moving from basic to acidic media. The intensity and sign of the signal around the π-π* region varies with the length of side chain; however no predictive trend was observed. CD spectra of **3T** compounds followed the similar pattern of crossover around the ICT and π-π* transitions (Figure 4b). In this case, spectra from basic and acidic environment did

not show much difference, further supporting the presence of assemblies in both media.

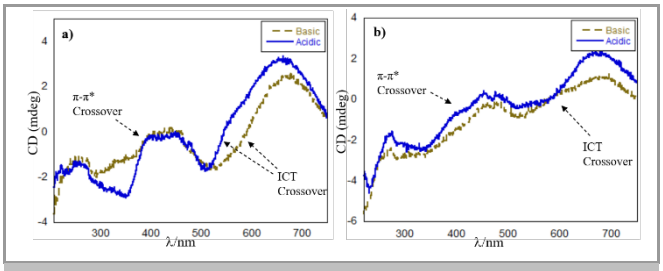

Figure 4 CD spectra of a) C1-2T and b) C1-3T molecules in basic and acidic solutions. All spectra were recorded at the 30-40 μM concentration range. Basic solutions were prepared by addition of 30 μL of KOH (1M) to the spectroscopic solution in water. Acidic samples were obtained by adding 80 μL of HCl (1M) to the basic sample.

Conclusions

We developed a novel synthetic methodology to incorporate the high performance DPP π-core to run linearly as a unique connectivity motif within peptidic backbones. We also varied the side-chain and number of thiophene units attached to the DPP-core to understand their influence in formation of self-assembled aggregates as manifested by several photophysical measurements (UV-vis, photoluminescence, CD). All of the peptides formed self-assembled structures as deduced from significant ICT blue-shifts and photoluminescence quenching. We observed that the variation of number of thiophene units has significant effect on the photophysical outcome, however, the side-chain variation does not alter the photophysical properties to a great extent. This study provides synthetic chemists an access to incorporate the DPP-cores into peptides in a new way. It also provides insight into the selection of appropriate chromophores and side chains to engineer the resulting optoelectronic and morphological properties.

Experimental Section

General Information

THF was acquired from an Innovative Technologies Pure Solv solvent purification system and dried over 4Å molecular sieves. Dimethylformamide (DMF) and diisopropylamine were purchased from Oakwood Products Inc. and dried over 4Å molecular sieves. N-Methyl-2-pyrrolidone (NMP) was obtained from Advanced ChemTech. Pyridine was obtained from Alfa-Aesar. Dichloromethane (DCM) was freshly distilled prior to storage. All solvents were stored over 4 Å molecular sieves and were subsequently degassed by sparging with nitrogen gas at least 30 min prior to use. Dimethyl succinate was purchased from Acros Organics. O-(Benzotriazol-1-yl)-N,N,N′N′-tetramethyluronium hexafluorophosphate (HBTU), 2-methyl-2-butanol, methyl iodide and 2-thiophenecarbonitrile were purchased from Oakwood Products Inc. Tetrakis(triphenylphosphine)palladium was obtained from Strem Chemicals. Wang resin (preloaded with amino acid) and Fmoc-protected amino acids were obtained from Advanced Chem Tech. Biotech grade cellulose ester dialysis tubing (MWCO 500-1000) was purchased from Spectrum Labs. All other reagents and starting materials were obtained from Sigma-Aldrich and were used as received. 5′-bromo-[2,2′-bithiophene]-5-carboxylic acid,[49] 3,6-di(thiophen-2-yl)-2,5-dihydropyrrolo[3,4-c]pyrrole-1,4-dione,[50] 2,5-bis(methyl)-3,6-di(thiophen-2-yl)pyrrolo[3,4-*c*]pyrrole-1,4(2*H*,5*H*)-dione,[51] 2,5-bis(butyl)-3,6-di(thiophen-2-yl)pyrrolo[3,4-*c*]pyrrole-1,4(2*H*,5*H*)-dione,[52] and 2,5-bis(butyl)-3,6-di(thiophen-2-yl)pyrrolo[3,4-*c*]pyrrole-1,4(2*H*,5*H*)-dione[53] were prepared according to previous reports.

Measurements and Characterization of Compounds

NMR Spectroscopy. ^{1}H-NMR spectra were obtained using a Bruker Advance 400 MHz FT-NMR spectrometer and processed with Bruker Topspin 1.3. Peptide ^{1}H NMR spectra were acquired using a presaturation pulse to suppress water. Chemical shifts are reported in parts per million relative to the residual protio solvent [HOD δ: 4.79, $CHCl_3$ δ: 7.26].

Electrospray Ionization Mass Spectrometry (ESI-MS). ESI samples were collected using a Thermo Finnigan LCQ Deca Ion Trap Mass Spectrometer in negative mode. Samples were prepared in a 1:1 MeOH:water solution with 1% ammonium hydroxide.

High Resolution Mass Spectrometry (HRMS). HRMS was performed on a VG-70SE Magnetic Sector Mass Spectrometer.

Reverse-Phase HPLC. HPLC purification was performed on an Agilent 1100 series (semipreparative/analytical) and a Varian PrepStar SD-1 (preparative) instrument using Luna 5 μm particle diameter C8 with TMS end-capping columns with silica solid support. An ammonium formate aqueous buffer (pH 8) and acetonitrile were used as the mobile phase.

UV–Vis and Photoluminescence. UV–vis spectra were obtained using a Varian Cary 50 Bio UV-vis spectrophotometer. Photoluminescence spectra were obtained using a PTi Photon Technology International Fluorometer (QuantaMaster 40) with a 75 W Ushio Xenon short arc lamp and operated with Felix32 Version 1.2 software. Peptide stock solutions were prepared at a *ca.* 1 mg/mL concentration (the exact molar concentration varied between 730-960 μM). Basic spectroscopic samples were prepared by adding 2955 μL of DI water, 20 μL of 1M KOH and 25 μL of the peptide stock sample. Acidic pH samples were prepared by rapid addition of 50 μL of 1M HCl to the basic pH sample.

Circular Dichroism (CD). CD spectra were obtained using a Jasco J-810 spectropolarimeter. Peptide stock solutions were prepared at a *ca.* 1 mg/mL concentration (the exact molar concentration varied between 730-960 μM). Basic spectroscopic samples were prepared by adding 2955 μL of DI water, 20 μL of 1M KOH and 125 μL of the peptide stock sample. Acidic pH samples were prepared by rapid addition of 50 μL of 1M HCl to the basic pH sample.

Dynamic Light Scattering (DLS). DLS data were obtained using a Zetasizer Nano-ZS90 (Malvern Instruments). Peptide stock solutions were prepared at a *ca.* 1 mg/mL concentration (the exact molar concentration varied between 730-960 μM). Basic spectroscopic samples were prepared by adding 2955 μL of DI water, 20 μL of 1M KOH and 25 μL of the peptide stock sample. Acidic pH samples were prepared by rapid addition of 50 μL of 1M HCl to the basic pH sample.

Transmission Electron Microscopy (TEM). Imaging was performed on a FEI Technai 12 TWIN transmission electron microscope equipped with an SIS Megaview III CCD digital camera at an accelerating voltage of 100 kV. Acidic solutions (0.1-0.075 wt %) of each peptide were prepared by placing the samples in a closed container with a vial of conc. HCl opened within, which initiated the assembly process by diffusion of HCl vapor to the sample. The peptides were pipetted (drop of 1 mg/mL solution) onto 200 mesh copper grids coated with carbon and incubated for 5 min at 25 °C. Excess solution was wicked off by touching the side of the grid to filter paper. The samples were then stained with a 2% uranyl acetate solution, and excess moisture was wicked off. The grid was allowed to dry in air before imaging.

Synthetic Procedures

General Solid-Phase Peptide Synthesis (SPPS). All peptides were synthesized using the standard Fmoc solid-phase technique with Wang resin preloaded with Fmoc-protected aspartic acid (Wang-Asp, 0.34 mmol/g). To the resin in a peptide chamber, Fmoc-deprotection was accomplished by adding a 20% piperidine solution in DMF twice (successive 5 and 10 min treatments) followed by washing with NMP × 3, methanol × 3, and DCM × 3. For the amino acid couplings, 3.0 equiv of the Fmoc-protected amino acid was activated with 2.9 equiv of HBTU and 10 equiv of diisopropylethylamine (DIPEA) in NMP, and this solution was added to the resin beads. The reaction mixture was allowed to mix for 45–90 min, after which the beads were rinsed with NMP, methanol, and DCM (3 times each). The completion of all couplings was monitored using

a Kaiser test on a few dry resin beads, repeating the same amino acid coupling as needed. The general procedure for amino acid coupling was repeated for each additional amino acid until the desired peptide sequence was obtained. The last amino acid was deprotected using piperidine solution leaving a -NH_2 terminated resin.

General N-acylation procedure for peptides. Following our previous procedure,[15] a solution containing 3 eq. of aryl halide carboxylic acid, HBTU (2.9 eq.) and DIPEA (10 eq.) was mixed for 3 h with the resin forming an N-acylated peptide capped with desired aryl halide. The completion of the couplings was assessed using a Kaiser test on a few dry resin beads. The resin was washed with NMP, methanol and DCM (3 times each).

*General DPP Core formation up to compound **2**.* 2-thiophenecarbonitrile (**1**) upon reacting with methyl ester of succinic acid forms the core in presence of a strong base like K-O^{t}Bu.[50] N-alkylation of the core (leading to **2**) was achieved in presence of a relatively weaker base such as K_2CO_3 under reflux condition.[51-53]

*General stannylation protocol leading to **3**.* These compounds were synthesized according to a modified literature procedure.[54] Compound **2** (0.300 mmol, 1 equiv.) was dissolved in 15 mL of anhydrous THF under N_2 atmosphere. The solution was cooled down to -78°C and 2.0 mL of freshly prepared LDA (lithium diisopropylamide) (0.900 mmol, 3 equiv., 0.45M in hexane) was added dropwise. The reaction mixture was allowed to come to 0°C over the course of 2 h, at which point it was stirred for an additional 2 h. Then the mixture was cooled to -78°C and trimethyltin chloride solution (1.05 mmol, 3.5 equiv., 1 M in hexane) was added rapidly. The mixture was allowed to come to room temperature and stirred overnight. The reaction was quenched with 15 mL of cold water and extracted with diethylether three times. It was further extracted with a potassium fluoride (1 M) solution three times and the organic layer was filtered through bed of celite. Finally, the organic layer was dried over anhydrous $MgSO_4$. After the removal of the solvent under vacuum, a purple solid was obtained that was used without further purification.

2,5-bis(methyl)-3,6-bis(5-(trimethylstannyl)thiophen-2-yl)-2,5-dihydropyrrolo[3,4-*c*]pyrrole-1,4-dione (**3a**)

Subjecting **2a** to the general procedure above provided **3a** (purple, solid). Yield: 0.159 g, 0.242 mmol, 80.7%.

^{1}H NMR (400 MHz, $CDCl_3$) δ: 8.99 (d, J = 3.68 Hz, 2H), 7.37 (d, J = 3.68 Hz, 2H), 3.65 (s, 6H), 0.45 (s, 18H).

HRMS (EI): calcd. for $C_{22}H_{28}N_2O_2S_2Sn_2$: 653.9630; found: 653.9644.

2,5-bis(butyl)-3,6-bis(5-(trimethylstannyl)thiophen-2-yl)-2,5-dihydropyrrolo[3,4-*c*]pyrrole-1,4-dione (3b)

Subjecting **2b** to the general procedure above provided **3b** (purple, solid). Yield: 0.166 g, 0.224 mmol, 74.7%.

^{1}H NMR (400 MHz, $CDCl_3$) δ: 9.00 (d, J = 3.60 Hz, 2H), 7.36 (d, J = 3.68 Hz, 2H), 4.13 (t, J = 7.40 Hz, 4H), 1.79-1.73 (m, 4H), 1.51-1.44 (m, 4H), 0.99 (t, J = 7.48 Hz, 6H), 0.47 (s, 18H).

HRMS (EI): calcd. for $C_{28}H_{40}N_2O_2S_2Sn_2$: 738.0569; found: 738.0569.

2,5-bis(hexyl)-3,6-bis(5-(trimethylstannyl)thiophen-2-yl)-2,5-dihydropyrrolo[3,4-*c*]pyrrole-1,4-dione (3c)

Subjecting **2c** to the general procedure above provided **3c** (purple, solid). Yield: 0.173 g, 0.217 mmol, 72.3%.

^{1}H NMR (400 MHz, $CDCl_3$) δ: 8.98 (d, J = 3.68 Hz, 2H), 7.34 (d, J = 3.68 Hz, 2H), 4.09 (t, J = 8.20 Hz, 4H), 1.76-1.71 (m, 4H), 1.46-1.41 (m, 4H), 1.34-1.32 (m, 8H), 0.89 (t, J = 7.12 Hz, 6H), 0.44 (s, 18H).

HRMS (EI): calcd. for $C_{32}H_{48}N_2O_2S_2Sn_2$: 794.1195; found: 794.1195.

General On-Resin Stille Coupling Procedure. The solid supported peptide resin capped with an aryl halide prepared as described above (1 equiv.) was transferred to a Schlenk flask equipped with a reflux condenser and dried under vacuum. $Pd(PPh_3)_4$ (4 mol%, relative to resin loading) was added to the reaction vessel. Approximately 0.5 equiv. of bis-stannylated aryl reagent **3** (0.50 eq) was added to the flask followed by approximately 10 mL of DMF via syringe. The mixture was heated to 80°C for 18 h and was agitated constantly by bubbling nitrogen through the solution. The mixture was allowed to cool to room temperature. The peptide was subjected to the general cleavage and work-up procedure described below to yield the crude product, then further purified by HPLC.

General Peptide Cleavage and Workup Procedure. Following dimerization, the resin was returned to the peptide chamber and again subjected to a standard wash cycle: 2 × NMP, 2 × methanol, and 2 × DCM. The resin was treated with 9.5 mL of trifluoroacetic acid, 250 µL of water, and 250 µL of triisopropylsilane for 3 h. The peptide solution was filtered from the resin beads, washed 3 times with DCM, and concentrated by evaporation under reduced pressure. The crude peptide was then precipitated from solution with 50−60 mL of diethyl ether and isolated through centrifugation. The resulting pellet was triturated with diethyl ether to yield crude product, which was dissolved in approximately 15−20 mL of water and 50 µL of potassium hydroxide (1 M) and lyophilized. The solution was placed inside dialysis tubing of the appropriate length. The tubing was stirred in 1 L of water for 1 h, the water was exchanged, and the tubing was allowed to stir for another 1 h. This process was repeated twice, and then the tubing was stirred overnight (approximately 15 h). The tubing was removed from water, and the peptide solution was transferred to a separate container and lyophilized.

C1-2T: Solid-supported Wang-EAA-NH_2 peptide N-acylated with 5-bromothiophene-2-carboxylic acid was prepared as described above (0.3 mmol). The peptide was coupled with 2,5-dimethyl-3,6-bis(5-(trimethylstannyl)thiophen-2-yl)-2,5-dihydropyrrolo[3,4-*c*]pyrrole-1,4-dione **3a** (0.15 mmol, 0.098 g) in the presence of $Pd(PPh_3)_4$ (0.012 mmol, 0.013 g) using the general on-resin Stille coupling procedure for 18 hours. Resin was then subjected to the general cleavage procedure, and the crude peptide **C1-2T** (dark purple, powder) was obtained (0.034 mmol, 0.038 g, 11% yield). Following HPLC purification, 0.0074 mmol, 0.0083 g, 2.5% yield.

MS (ESI) m/z 1121.5 $(M-H)^-$ (calc. 1122.2), m/z, m/z 560.28 $(M-2H)^{2-}$ (calc. 560.61).

C4-2T: Solid-supported Wang-EAA-NH_2 peptide N-acylated with 5-bromothiophene-2-carboxylic acid was prepared (0.3 mmol). The peptide was coupled with 2,5-dibutyl-3,6-bis(5-(trimethylstannyl)thiophen-2-yl)-2,5-dihydropyrrolo[3,4-*c*]pyrrole-1,4-dione **3b** (0.15 mmol, 0.11 g) in the presence of $Pd(PPh_3)_4$ (0.012 mmol, 0.013 g) using the general on-resin Stille coupling procedure for 18 hours. Resin was then subjected to the general cleavage procedure and crude peptide **C4-2T** (dark purple, powder) was obtained (0.034 mmol, 0.041 g, 11% yield). Following HPLC purification, 0.0073 mmol, 0.0088 g, 2.4% yield.

MS (ESI) m/z 1206.1 $(M-H)^-$ (calc. 1206.4), m/z 602.23 $(M-2H)^{2-}$ (calc. 602.71).

C6-2T: Solid-supported Wang-EAA-NH_2 peptide N-acylated with 5-bromothiophene-2-carboxylic acid was prepared (0.3 mmol). The peptide was coupled with 2,5-dihexyl-3,6-bis(5-(trimethylstannyl)thiophen-2-yl)-2,5-dihydropyrrolo[3,4-*c*]pyrrole-1,4-dione **3c** (0.15 mmol, 0.12 g) in the presence of $Pd(PPh_3)_4$ (0.012 mmol, 0.013 g) using the general on-resin Stille coupling procedure for 18 hours. Resin was then subjected to the general cleavage procedure and crude peptide **C6-2T** (dark purple, powder) was obtained (0.026 mmol, 0.034 g, 9.0% yield). Following HPLC purification, 0.0045 mmol, 0.0057 g, 1.5% yield.

MS (ESI) m/z 649.21 $(M+K-3H)^{2-}$ (calc. 649.73), m/z 630.24 $(M-2H)^{2-}$ (calc. 630.33).

C1-3T: Solid-supported Wang-EAA-NH_2 peptide N-acylated with 5'-bromo-[2,2'-bithiophene]-5-carboxylic acid was prepared (0.3 mmol). The peptide was coupled with 2,5-dimethyl-3,6-bis(5-(trimethylstannyl)thiophen-2-yl)-2,5-dihydropyrrolo[3,4-*c*]pyrrole-1,4-dione **3a** (0.15 mmol, 0.10 g) in the presence of $Pd(PPh_3)_4$ (0.012 mmol, 0.013 g) using the general on-resin Stille coupling procedure for 18 hours. Resin was then subjected to the general cleavage procedure and crude peptide **C1-3T** (dark purple, powder) was obtained (0.033 mmol, 0.042 g, 11% yield). Following HPLC purification, 0.0048 mmol, 0.0062 g, 1.6% yield.

MS (ESI) m/z 1286.5 $(M-H)^-$ (calc. 1286.5), m/z 642.4 $(M-2H)^{2-}$ (calc. 642.76).

C6-3T: Solid-supported Wang-EAA-NH_2 peptide N-acylated with 5'-bromo-[2,2'-bithiophene]-5-carboxylic acid was prepared (0.3 mmol). The peptide was coupled with 2,5-dihexyl-3,6-bis(5-(trimethylstannyl)thiophen-2-yl)-2,5-dihydropyrrolo[3,4-*c*]pyrrole-1,4-dione **3c** (0.15 mmol, 0.12 g) in the presence of $Pd(PPh_3)_4$ (0.012 mmol, 0.013 g) using the general on-resin Stille coupling procedure for 18 hours. Resin was then subjected to the general cleavage procedure and crude peptide **C6-3T** (dark purple, powder) was obtained (0.022 mmol, 0.031 g, 7.2% yield). Following HPLC purification, 0.0041 mmol, 0.0059 g, 1.4% yield.

MS (ESI) m/z 1464.6 $(M+K-2H)^-$ (calc. 1464.7), m/z 731.30 $(M+K-3H)^{2-}$ (calc. 731.86), m/z 712.85 $(M-2H)^{2-}$ (calc. 712.86).

Funding Information

This research is based upon work supported by the National Science Foundation's Designing Materials to Revolutionize and Engineer our Future (DMREF) program (Grant Nos. DMR-1728947).

Acknowledgment

We acknowledge support from Johns Hopkins University. We thank the Center for Molecular Biophysics (JHU) for the use of a circular dichroism spectrometer, and Prof. Hai-Quan Mao for the use of a Zetasizer for the dynamic light scattering experiments.

Supporting Information

YES (this text will be updated with links prior to publication)

Primary Data

NO (this text will be deleted prior to publication)

References

(1) Palmer, L. C.; Stupp, S. I. *Acc. Chem. Res*. **2008**, *41*, 1674.
(2) Gazit, E. *Chem. Soc. Rev*., **2007**, *36*, 1263.
(3) Fleming, S.; Ulijn, R. V. *Chem. Soc. Rev*. **2014**, *43*, 8150.
(4) Hamley, I. W. *Angew. Chem., Int. Ed*. **2014**, *53*, 6866.
(5) Tovar, J. D. *Acc. Chem. Res*. **2013**, *46*, 1527.
(6) Panda, S. S.; Katz, H. E.; Tovar, J. D. *Chem. Soc. Rev*. **2018**, *47*, 3640.
(7) Kas, O. Y.; Charati, M. B.; Rothberg, L. J.; Galvin, M. E.; Kiick, K. L. *J. Mater. Chem*., **2008**, *18*, 3847.
(8) Matmour, R.; De Cat, I.; George, S. J.; Adriaens, W.; Leclère, P.; Bomans, P. H. H.; Sommerdijk, N. A. J. M.; Gielen, J. C.; Christianen, P. C. M.; Heldens, J. T.; van Hest, J. C. M.; Löwik, D. W. P. M.; De Feyter, S.; Meijer, E. W.; Schenning, A. P. H. J. *J. Am. Chem. Soc*. **2008**, *130*, 14576.
(9) Zhou, J., Du, X., Gao, Y., Shi, J., and Xu, B. *J. Am. Chem. Soc*. **2014**, *136*, 2970.
(10) Adhikari, B., Nanda, J., and Banerjee, A. *Chem. - Eur. J.* **2011**, *17*, 11488.
(11) Khalily, M. A.; Bakan, G.; Kucukoz, B.; Topal, A. E.; Karatay, A.; Yaglioglu, H. G.; Dana, A.; Guler, M. O. *ACS Nano* **2017**, *11*, 6881.
(12) Draper, E. R.; Walsh, J. J.; McDonald, T. O.; Zwijnenburg, M. A.; Cameron, P. J.; Cowan, A. J.; Adams, D. J. *J. Mater. Chem. C* **2014**, *2*, 5570.
(13) Schillinger, E.-K.; Mena-Osteritz, E.; Hentschel, J.; Börner, H. G.; Bäuerle, P. *Adv. Mater*. **2009**, *21*, 1562.
(14) Tsai, W. W.; Tevis, I. D.; Tayi, A. S.; Cui, H.; Stupp, S. I. *J. Phys. Chem. B* **2010**, *114*, 14778.
(15) Panda, S. S.; Shmilovich, K.; Ferguson, A. L.; Tovar, J. D. *Langmuir* **2019**, *35*, 14060.
(16) Wall, B. D.; Zacca, A. E.; Sanders, A. M.; Wilson,W. L.; Ferguson, A. L.; Tovar, J. D. *Langmuir* **2014**, *30*, 5946.
(17) Lee, T.; Panda, S. S.; Tovar, J. D.; Katz, H. E. *ACS Nano* **2020**, *14*, 1846.
(18) Sanders, A. M.; Kale, T. S.; Katz, H. E.; Tovar, J. D. *ACS Omega* **2017**, *2*, 409.
(19) Wall, B. D.; Diegelmann, S. R.; Zhang, S. M.; Dawidczyk, T. J.; Wilson, W. L.; Katz, H. E.; Mao, H. Q.; Tovar, J. D. *Adv. Mater*., **2011**, *23*, 5009.
(20) Kale, T. S.; Tovar, J. D. *Tetrahedron* **2016**, *72*, 6084.
(21) Kale, T. S.; Ardona, H. A. M.; Ertel, A.; Tovar, J. D. *Langmuir* **2019**, *35*, 2270.
(22) Tamayo, A. B.; Walker, B.; Nguyen, T-C. *J. Phys. Chem. C* **2008,** *112,* 11545.
(23) Aytun, T.; Santos, P. J.; Bruns, C. J.; Huang, D.; Koltonow, A. R.; Cruz, M. O. D.; Stupp, S. I. *J. Phys. Chem. C* **2016**, *120*, 3602.
(24) Kanimozhi, C.; Yaacobi-Gross, N.; Chou, K. W.; Amassian, A.; Anthopoulos, T. D.; Patil, S. *J. Am. Chem. Soc.* **2012**, *134*, 16532.
(25) Sonar, P.; Singh, S. P.; Li, Y.; Soh, M. S.; Dodabalapur, A. *Adv. Mater*. **2010**, *22*, 5409.
(26) Bijleveld, J. C.; Zoombelt, A. P.; Mathijssen, S. G. J.; Wienk, M. M.; Turbiez, M.; Leeuw, D. M.; Janssen, R. A. J. *J. Am. Chem. Soc*. **2009**, *131*, 16616.
(27) Tang, A.; Zhan, C.; Yao, J.; Zhou, E. *Adv. Mater*. **2017**, *29*, 1600013.
(28) Iqbal, A.; Cassar, L.; Rochat, A. C.; Pfenninger, J. *J. Coat. Technol.***1988**, *60*, 37.
(29) Nielsen, C. B.; Turbiez, M.; McCulloch, I. *Adv. Mater*. **2013**, *25*, 1859.
(30) Ley, D.; Guzman, C.; Adolfsson, K. H.; Scott, A. M.; Braunschweig, A. B. *J. Am. Chem. Soc*. **2014**, *136*, 7809.
(31) Zhang, X.; Richter, L. J.; DeLongchamp, D. M.; Kline, R. J.; Hammond, M. R.; McCulloch, I.; Heeney, M.; Ashraf, R. S.; Smith, J. N.; Anthopoulos, T. D.; Schroeder, B.; Geerts, Y. H.; Fischer, D. A.; Toney, M. F. *J. Am. Chem. Soc*., **2011**, *133*, 15073.
(32) Back, J. Y.; Yu, H.; Song, I.; Kang, I.; Ahn, H.; Shin, T. J.; Kwon, S.-K.; Oh, J. H.; Kim, Y.-H. *Chem. Mater*., **2015**, *27*, 1732.
(33) Gruber, M.; Jung, S.-H.; Schott, S.; Venkateshvaran, D.; Kronemeijer, A. J.; Andreasen, J. W.; McNeill, C. R.; Wong, W. W. H.; Shahid, M.; Heeney, M.; Lee, J.-K.; Sirringhaus, H. *Chem. Sci*. **2015**, *6*, 6949.
(34) Grzybowski, M.; Gryko, D. T. *Adv. Optical Mater*. **2015**, *3*, 280.
(35) Tamayo, A. B.; Tantiwiwat, M.; Walker, B.; Nguyen, T-C. *J. Phys. Chem. C* **2008**, *112*, 15543.
(36) Stolte, M.; Suraru, S-L.; Diemer, P.; He, T.; Burschka, C.; Zschieschang, U.; Klauk, H.; Würthner, F. *Adv. Funct. Mater*. **2016**, *26*, 7415.
(37) Draper, E. R.; Dietrich, B.; Adams, D. J. *Chem. Commun*., **2017**, *53*, 1864.
(38) Rani, A.; Kavianinia, I.; Hume, P.; Leon-Rodriguez, L. M. D.; Kihara, S.; Williams, D. E.; McGillivray, D. J.; Plank, N. O. V.; Gerrard, J.; Hodgkiss, J. M.; Brimble, M. A. *Soft Matter*, **2020**, *16*, 6563.
(39) Ftouni, H.; Bolze, F.; Roquigny, H. de; Nicoud, J.-F. *Bioconjugate Chem*. **2013**, *24*, 942.
(40) Ftouni, H.; Bolze, F.; Nicoud, J.-F. *Dyes Pigm*. **2013**, *97*, 77.
(41) Heyer, E.; Lory, P.; Leprince, J.; Moreau, M.; Romieu, A.; Guardigli, M.; Roda, A.; Ziessel, R. *Angew. Chem., Int. Ed*., **2015**, *54*, 2995.
(42) Zhang, G.; Li, H.; Bi, S.; Song, L.; Lu, Y.; Zhang, L.; Yu, J.; Wang, L. *Analyst* **2013**, *138*, 6163
(43) Zhang, G.; Song, L.; Bi, S.; Wu, Y.; Yu, J.; Wang, L. *Dyes Pigm*. **2014**, *102*, 100.
(44) Besar, K. Ardona, H. A. M.; Ertel, A.; Tovar, J. D. *ACS Nano*, **2015**, *9*, 12401.
(45) Farahat, M.; Wei, H.-Y.; Ibrahem, M. A.; Boopathi, K. M.; Wei, K.-H.; Chu, C.-W. *RSC Adv*. **2014**, *4*, 9401.
(46) Szabadai, R. S.; Roth-Barton, J.; Ghiggino, K. P.; White, J. M.; Wilson, D. J. D. *Aust. J. Chem*. **2014**, *67*, 1330.
(47) Mei, J.; Graham, K. R.; Stalder, R.; Tiwari, S. P.; Cheun, H.; Shim, J.; Yoshio, M.; Nuckolls, C.; Kippelen, B.; Castellano, R. K.; Reynolds, J. R. *Chem. Mater*. **2011**, *23*, 2285.
(48) Naik, M. A.; Venkatramaiah, N.; Kanimozhi, C.; Patil, S. *J. Phys. Chem. C* **2012**, *116*, 26128.
(49) Kilbinger, A. F. M.; Schenning, A. P. H. J.; Goldoni, F.; Feast, W. J.; Meijer, E. W. *J. Am. Chem. Soc*. **2000**, *122*, 1820.
(50) Sonar, P.; Singh, S. P.; Li, Y.; Ooi, Z.-E.; Ha, T.; Wong, I.; Soh, M. S.; Dodabalapur, A. *Energy Environ. Sci*., **2011**, *4*, 2288.
(51) Stas, S.; Sergeyev, S.; Geerts, Y. *Tetrahedron*, **2010**, *66*, 1837.
(52) Zhou, E.; Wei, Q.; Yamakawa, S.; Zhang, Y.; Tajima, K.; Yang, C.; Hashimoto, K. *Macromolecules*, **2010**, *43*, 821.

(53) Tamayo, A. B.; Tantiwiwat, M.; Walker, B.; Nguyen, T-C. *J. Phys. Chem. C* **2008,** *112,* 15543.
(54) Fu, L.; Fu, W.; Cheng, P.; Xie, Z.; Fan, C.; Shi, M.; Ling, J.; Hou, J.; Zhan, X.; Chen, H. *J Mater Chem A* **2014**, *2*, 6589.